

Citric based sol-gel synthesis and photoluminescence properties of un-doped and Sm^{3+} doped $\text{Ca}_3\text{Y}_2\text{Si}_3\text{O}_{12}$ phosphors

Vengala Rao Bandi^a, Bhaskar Kumar Grandhe^a, Kiwan Jang^{a,*}, Ho-Sueb Lee^a,
Soung-Soo Yi^b, Jung-Hyun Jeong^c

^a Department of Physics, Changwon National University, Changwon, Republic of Korea

^b Department of Photonics, Silla University, Busan, Korea

^c Department of Physics, Pukyong National University, Busan, Korea

Received 29 November 2010; received in revised form 29 December 2010; accepted 24 February 2011

Available online 8 April 2011

Abstract

The photoluminescent properties of un-doped and Sm^{3+} doped $\text{Ca}_3\text{Y}_2\text{Si}_3\text{O}_{12}$ phosphors were prepared by the citrate sol-gel method. Un-doped sample has shown a strong blue emission, which has its maximum intensity at 389 nm. Among all the observed emission transitions $^4\text{G}_{5/2} \rightarrow ^6\text{H}_J$ ($J = 5/2, 7/2 \text{ \& } 9/2$) of Sm^{3+} , the reddish-orange (RO) emission transition $^4\text{G}_{5/2} \rightarrow ^6\text{H}_{7/2}$ is more prominent, which matches well with the emission wavelength of near UV (n-UV) LED. The reasons for the observance of such prominent visible color emissions from these phosphors have been substantiated appropriately. Besides, structural details of these samples have also been analyzed from the measured XRD, TEM, TG-DTA and FT-IR profiles.

© 2011 Elsevier Ltd and Techna Group S.r.l. All rights reserved.

Keywords: A. Sol-gel process; B. Spectroscopy; C. Optical Properties; Color

1. Introduction

White light emitting diodes (WLEDs) are considered to be the next generation light source as a consequence of their efficiency, lifetime, low environmental impact than incandescent or fluorescent lamps [1,2]. The first commercial WLED, produced by Nichia Corporation was fabricated by combining the blue emission of GaN based diode chip with the yellow luminescence from $\text{Y}_3\text{Al}_5\text{O}_{12}:\text{Ce}^{3+}$ (YAG:Ce) phosphor [3]. However, the shortcomings in this YAG based WLEDs are poor color rendering that arise due to lack of orange & red components and seriously thermal quenching luminescence [4–6]. As an alternative, combining red, green, and blue phosphors with n-UV GaN based diode chips to produce white light is highly favored. The most common red-emitting phosphor used in these WLEDs is the $\text{Y}_2\text{O}_2\text{S}:\text{Eu}^{3+}$. However, it suffers from disadvantages like low luminous efficiency compared with its counterpart blue ($\text{BaMgAl}_{10}\text{O}_{17}:\text{Eu}^{2+}$) and

green ($\text{ZnS}:\text{Cu}^+, \text{Al}^{3+}$) phosphors [7,8]. To overcome its low efficiency, a large amount of $\text{Y}_2\text{O}_2\text{S}:\text{Eu}^{3+}$ had to be used in comparison with the blue and green phosphors. Therefore, a lot of research effort is directed to find an alternative red phosphor which exhibited the intense red emission with the excitation band around 400 nm, for n-UV LED chips.

In the process of identifying novel and efficient materials for red emissive displays, selection of host materials is an essential issue. The emission spectra of rare-earth (RE) ions almost remain the same in different hosts, but the luminescent efficiency, chemical stability and durability largely depend on the physical properties of the host matrix. Recently, RE ions doped in silicate based host matrices have been attracting the attention of several research groups due to the demonstration of their enhanced optical properties over other existing systems [9,10]. Keeping in view of this above useful essentials, we have chosen $\text{Ca}_3\text{Y}_2\text{Si}_3\text{O}_{12}$ as a host matrix for the present investigation. The $\text{Ca}_3\text{Y}_2\text{Si}_3\text{O}_{12}$ does not crystallize in the garnet-type structure, also it is partly disordered from the garnet structure but in the iso-structure with $\text{Ca}_5(\text{PO}_4)_2\text{SiO}_4$ [11]. In order to emphasize the significance of the present host matrix, we have prepared and analyzed its photoluminescence

* Corresponding author. Tel.: +82 55 213 3425; fax: +82 55 267 0263.

E-mail address: kwjang@changwon.ac.kr (K. Jang).

properties with and without any dopant and we have thus elucidated the role of the undertaken host matrix in demonstrating such potential red emission from the Sm^{3+} doped $\text{Ca}_3\text{Y}_2\text{Si}_3\text{O}_{12}$ phosphor. As far as our knowledge is concerned, this has not been reported before.

2. Experimental

$\text{Ca}_3\text{Y}_{2-x}\text{Sm}_x\text{Si}_3\text{O}_{12}$ ($x = 0, 0.005, 0.01, 0.03$ & 0.05) samples were prepared by adopting citrate based sol-gel method. Stoichiometric amounts of CaCO_3 , Y_2O_3 , Sm_2O_3 (99.99%) and tetraethyl-ortho-silicate (TEOS) were taken as starting materials. CaCO_3 , RE_2O_3 were first dissolved in nitric acid then mixed with a double distilled water and ethanol (volume ratio = 1:4) solution. Afterwards, Citric acid (AR grade) was added to the above solution as chelating agent for the metal ions. The molar ratio of metal ions to citric acid was maintained in the ratio of 1:2, subsequently TEOS was added to this solution and stirred well. Ammonia was added to the above solution that neutralizes the excess nitrate content. The gel thus formed was kept in an oven at 100°C for drying and the resulting powders were put into a furnace for pre-calcination at 400°C for 3h and then sintered at 1000°C for 6h to obtain the phosphor samples.

The phase identification of the prepared samples were carried out by powder x-ray diffraction (XRD) using a Rigaku D/max x-ray Diffractometer with $\text{Cu-K}\alpha$ radiation ($\lambda = 1.5406\text{\AA}$), the operational voltage and current were maintained at 30 kV and 20 mA, respectively. Transmission electron microscope (TEM, JEOL JEM-2010) was used to examine the particle morphology. Thermogravimetry (TG) and Differential thermal analysis (DTA) were measured by using Netzsch STA 409 Simultaneous Thermal Analyzer with the precursor in N_2 atmosphere with a heating rate of $10^\circ\text{C}/\text{min}$. FTIR spectra of the phosphor samples were recorded on a Jasco FTIR-200 E spectrometer with KBr pellet technique from 4000 cm^{-1} to 400 cm^{-1} . The photoluminescence (PL) spectra of these phosphors were recorded on the Hitachi F-7000 fluorescence spectrometer. All the characterizations were performed at room temperature.

3. Results and Discussion

Fig. 1. shows the XRD patterns of $\text{Ca}_3\text{Y}_2\text{Si}_3\text{O}_{12}$ and $\text{Ca}_3\text{Y}_{1.97}\text{Sm}_{0.03}\text{Si}_3\text{O}_{12}$ phosphors. The obtained diffraction patterns are well indexed with orthorhombic structure (space group $Pnma$) and are consistent with the standard JCPDS-87-0453. In the prepared phosphor, it is noticed that the trivalent yttrium site is substituted by the trivalent samarium ions due to the similar ionic radius of Sm^{3+} (0.096nm) and Y^{3+} (0.093nm). These results confirms that the Sm^{3+} is clearly substituted into Y^{3+} without disturbing the host lattice and the obtained product has no detectable amount of impurity. The crystallite size of the prepared ceramic phosphor has been estimated using the Scherrer's equation:

$$D = 0.9\lambda / \beta \cos\theta$$

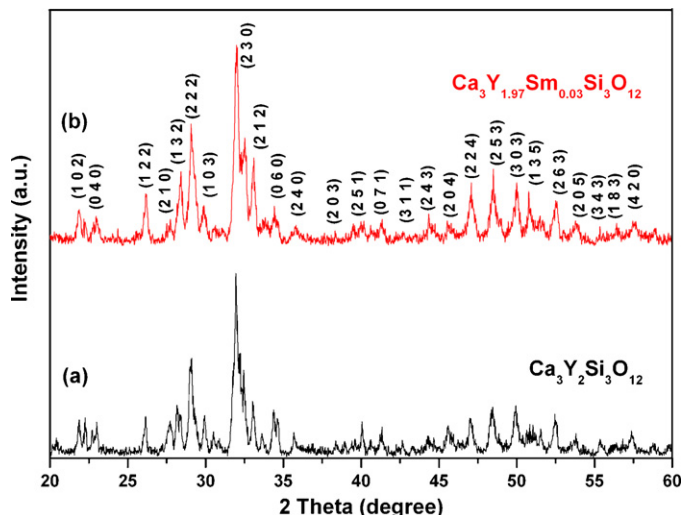


Figure 1. XRD patterns of (a) $\text{Ca}_3\text{Y}_2\text{Si}_3\text{O}_{12}$ (b) $\text{Ca}_3\text{Y}_{1.97}\text{Sm}_{0.03}\text{Si}_3\text{O}_{12}$ phosphors sintered at 1000°C .

where D is the crystallite size, λ is the X-ray wavelength (0.15405 nm), θ and β are the diffraction angle and full width at half maximum (FWHM) of an observed peak respectively. Intense diffraction peaks have been selected to compute the crystallite size and it is found to be in an average size of 72 nm . The TEM image of the $\text{Ca}_3\text{Y}_{1.97}\text{Sm}_{0.03}\text{Si}_3\text{O}_{12}$ phosphor sintered at 1000°C is shown in Fig. 2. From the figure, we observed that the heat treatment of the reaction mixture at 1000°C resulted in the formation of a powder having a complex morphology; it consists of a blend of sub micrometer-sized spherical particles (dark color) and irregular grey particles, which are non-uniformly spread over the surface of the dark particles. The average diameter of the particles is less than 200 nm , as estimated from a micrograph.

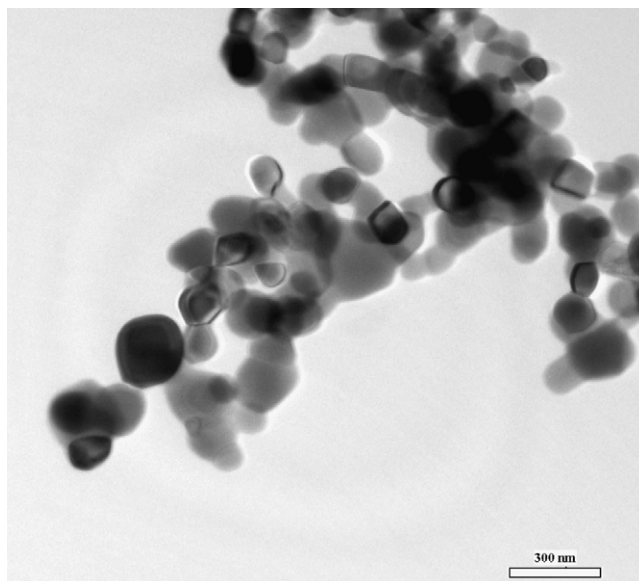


Figure 2. TEM image of $\text{Ca}_3\text{Y}_{1.97}\text{Sm}_{0.03}\text{Si}_3\text{O}_{12}$ phosphor.

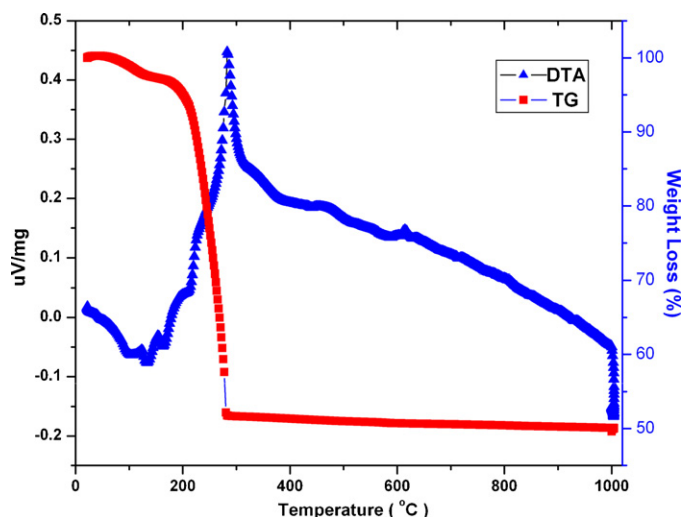


Figure 3. DTA-TG curves of $\text{Ca}_3\text{Y}_{1.97}\text{Sm}_{0.03}\text{Si}_3\text{O}_{12}$ precursors.

Fig. 3 shows the TG-DTA curves of precursor for $\text{Ca}_3\text{Y}_{1.97}\text{Sm}_{0.03}\text{Si}_3\text{O}_{12}$ phosphor. The TG curve has shown three stages of weight loss. The first stage of weight loss of about 11% is observed between 20 °C and 215 °C, accompanied by three endothermic peaks at 135, 164 and 215 °C in the DT curve due to the evaporation of residual ethanol and water in the gel. The second stage of weight loss (38%) is became faster from 215 °C to 290 °C, accompanied by a strong exothermic peak at 285 °C in DT curve is occurred due to the burnout of excess solvents [12,13]. The slight weight loss observed above 290 °C is attributed to the loss of CO content present in the sample. A weak exothermic peak which could be noticed above 600 °C in the DT curve is due to the crystallization of the precursor. The IR spectra presented in Fig. 4 shows the product sintered at 1000 °C. The IR absorption

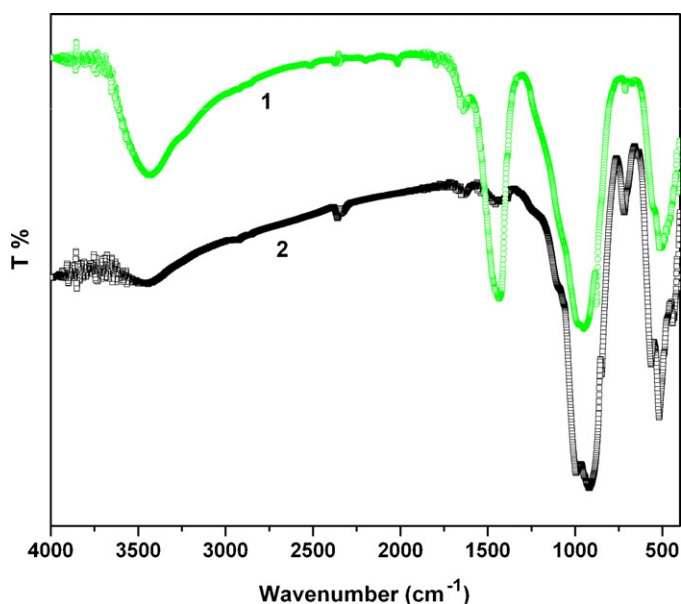


Figure 4. FTIR spectra of the $\text{Ca}_3\text{Y}_{1.97}\text{Sm}_{0.03}\text{Si}_3\text{O}_{12}$ phosphors. (1) Precursor (2) sintered at 1000 °C.

due to tetrahedral SiO_4 units can be assigned based on four kinds of modes consisting of ν_1 (symmetric stretching), ν_2 (symmetric bending), ν_3 (anti symmetric stretching) and ν_4 (anti symmetric bending). The bands noticed in the region of 400–1300 cm^{-1} are due to the stretching and bending modes of silicate bonds. As seen in figure the stretching vibrations of SiO_4 units (ν_1 and ν_3) has resulted fairly intense and broad absorption bands in the region of 800–1130 cm^{-1} . The bending vibrations (ν_2 and ν_4) of the SiO_4 unit have shown absorption bands observed at 400 and 600 cm^{-1} . The peak noticed at 565 cm^{-1} is due to the bending vibrations of Y–O bond. However, we noticed some insignificant bands near 1680 cm^{-1} , 2921 cm^{-1} and 3432 cm^{-1} that are associated to the OH content adsorbed at the powder surface when the sample was in contact with the environment during the preparation process of measurement. All the assignments thus made for $\text{Ca}_3\text{Y}_{1.97}\text{Sm}_{0.03}\text{Si}_3\text{O}_{12}$ phosphors and the obtained results are found to be quite well comparable with the results reported in literature [14,15].

Fig. 5 shows, the excitation spectrum of un-doped $\text{Ca}_3\text{Y}_2\text{Si}_3\text{O}_{12}$ phosphor and it presented a tiny broadband centered at 245 nm when the emitted signal was at 389 nm. The corresponding un-doped emission spectrum is shown in Fig. 5 which is monitored with an excitation wavelength of 245 nm and a broad band signal emitted with the maximum intensity centered at 389 nm was obtained due to the disordered structure of the $\text{Ca}_3\text{Y}_2\text{Si}_3\text{O}_{12}$. The disorder originates from the distribution of both divalent (Ca^{2+}) and trivalent (Y^{3+}) cations over the nine-eight-and-seven-coordinated sites of the silico-carnotite structure [11]. However, the occurrence of emission in $\text{Ca}_3\text{Y}_2\text{Si}_3\text{O}_{12}$ is expected to make relaxation process of the Ln^{3+} excited states. It is produced by the non-radiative relaxation of one electron, excited from the valence to the conductive band, to one luminescent recombination site and then the luminescent relaxation to the valence band. The broad bandwidth indicates the existence of a recombination band within the bandgap of the

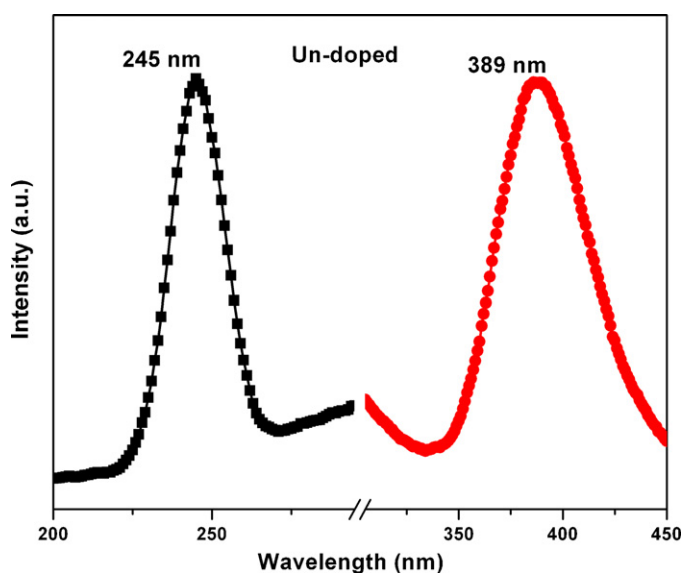


Figure 5. PLE and Emission spectra of $\text{Ca}_3\text{Y}_2\text{Si}_3\text{O}_{12}$.

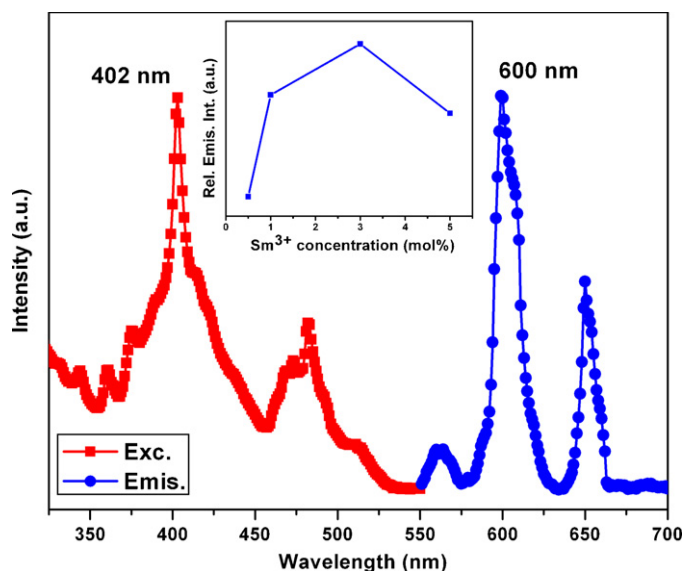


Figure 6. PLE and Emission spectra of $\text{Ca}_3\text{Y}_{1.97}\text{Sm}_{0.03}\text{Si}_3\text{O}_{12}$ phosphor and Inset shows RO emission intensity of $\text{Ca}_3\text{Y}_{2-x}\text{Sm}_x\text{Si}_3\text{O}_{12}$ ($x = 0.005, 0.01, 0.03$ & 0.05) phosphors.

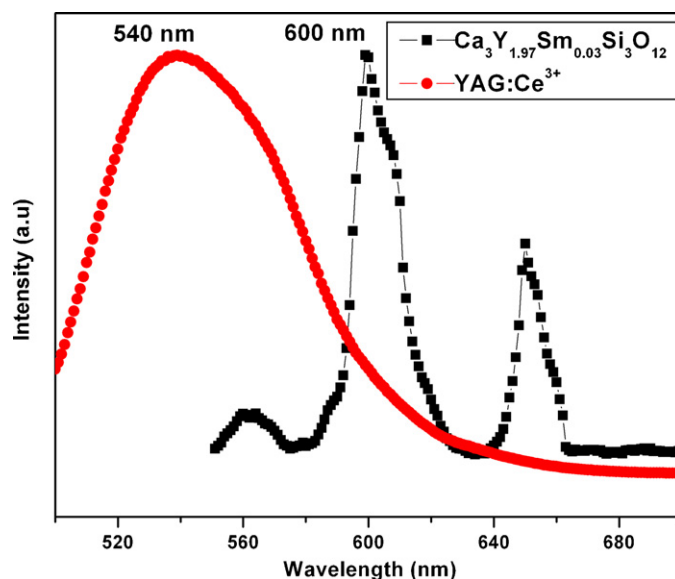


Figure 7. Typical photoluminescence spectra of $\text{Ca}_3\text{Y}_{1.97}\text{Sm}_{0.03}\text{Si}_3\text{O}_{12}$ and YAG:Ce^{3+} phosphors.

host. Fig. 6 shows the excitation spectrum of $\text{Ca}_3\text{Y}_{1.97}\text{Sm}_{0.03}\text{Si}_3\text{O}_{12}$ phosphor and it reveals that many excitation peaks are noticed in the wavelength region 325–525 nm with the intense excitation peak at 402 nm, which is perfectly matching with the emission wavelength of n-UV LED. Using 402 nm as the excitation wavelength, we have recorded the emission spectrum of $\text{Ca}_3\text{Y}_{1.97}\text{Sm}_{0.03}\text{Si}_3\text{O}_{12}$ phosphor and it has been shown in Fig. 6. Referring to the published papers, the measured emission bands at 562, 600, 650 nm have properly been assigned to the electronic transitions of $^4\text{G}_{5/2} \rightarrow ^6\text{H}_{5/2,7/2,9/2}$ respectively [16,17]. Among them, the intense RO color emitting transition is $^4\text{G}_{5/2} \rightarrow ^6\text{H}_{7/2}$ (600 nm) which obeys the selection rule of $\Delta J = \pm 1$ indicating it as a magnetic dipole (MD) and allowed transition but it is an electric dipole (ED) dominated. Therefore, it can be stated as it is partly a MD and partly an ED natured transition. The other transition $^4\text{G}_{5/2} \rightarrow ^6\text{H}_{9/2}$ is purely an ED transition which is sensitive to the crystal field and $^4\text{G}_{5/2} \rightarrow ^6\text{H}_{9/2}$ is MD transition [18]. Generally, the intensity ratio of ED to MD transitions could be used to understand the symmetry of the local environment of the trivalent 4f ions in the host matrix investigated. The greater the intensity of the ED transition, more the asymmetric nature. In the present work $^4\text{G}_{5/2} \rightarrow ^6\text{H}_{9/2}$ transition of Sm^{3+} ions have been measured to be quite intense than the MD transition $^4\text{G}_{5/2} \rightarrow ^6\text{H}_{5/2}$ which describes the asymmetric nature of host matrix investigated. From the Figs. 5 and 6, we observed a clear overlapping between the emission spectrum of the un-doped sample with the excitation spectrum of the Sm^{3+} doped sample and this result clearly demonstrates that there exists some kind of energy transfer from the host to the activator ion [19]. That is, once the host absorbs the pumping energy it emits a single band centered at 389 nm. When Sm^{3+} ions are present in host lattices, the excitation energy can be non-radiatively transferred to Sm^{3+} ion, resulting in its characteristic emission. From the recorded PL spectra, the intensity and color coordinate of the phosphor

were significantly influenced with an increase in the Sm^{3+} dopant concentration. The relation between RO emission intensity and Sm^{3+} concentration is shown in the inset of Fig. 6. It is well known that photon emission intensity of RE activator ions exhibits an optimum concentration in phosphor materials and it is hard to create efficient emission when the RE activator ions concentration is too low. On the other hand, the cross-relaxation interaction between the nearest RE activator ions will quench the emission if the RE activator ions exceed its optimum content. The experimental results revealed that the emission intensity of $\text{Ca}_3\text{Y}_2\text{Si}_3\text{O}_{12}$ increased with the Sm^{3+} concentration. The emission intensity reached to its maximum when the concentration of Sm^{3+} was 3 mol% and then decreased with concentration because thereafter the increase of Sm^{3+} concentration increases the cross-relaxation between two neighboring Sm^{3+} ions and hence it quenches the emission intensity. The process of cross-relaxation is due to non-radiative electric dipole–electric quadrupole transition from the $^4\text{G}_{5/2}$ energy level. In general, color is represented by means of color coordinates. Hence, in our present work, the chromaticity coordinates of $\text{Ca}_3\text{Y}_{1.97}\text{Sm}_{0.03}\text{Si}_3\text{O}_{12}$ phosphor have been calculated from the emission spectra and its color coordinates are found to be having a numerical value of (0.592, 0.402).

The typical PL spectra of the $\text{Ca}_3\text{Y}_{1.97}\text{Sm}_{0.03}\text{Si}_3\text{O}_{12}$ phosphor along with the emission spectra of standard YAG:Ce^{3+} phosphor was shown in Fig. 7. The YAG:Ce^{3+} phosphor can be effectively excited by the 470 nm blue light and emits strong yellow emission at 540 nm. The white light realized by the combination with a blue LED exhibits a poor color rendering index due to the lack of red color component. Hence for the phosphor sample undertaken here, the emission of $\text{Ca}_3\text{Y}_{1.97}\text{Sm}_{0.03}\text{Si}_3\text{O}_{12}$ phosphor occurs at a fairly longer wavelength at 600 nm under the excitation wavelength of 402 nm, which perfectly matches with the emission wavelengths of n-UV GaN based LEDs. The results suggest that

Sm^{3+} in $\text{Ca}_3\text{Y}_2\text{Si}_3\text{O}_{12}$ is an efficient RO emitting phosphor for WLEDs to resolve its shortcoming of deficiency in red component.

4. Conclusion

In conclusion, $\text{Ca}_3\text{Y}_{2-x}\text{Sm}_x\text{Si}_3\text{O}_{12}$ ($x = 0.005, 0.01, 0.03$ & 0.05) phosphors were prepared by adapting the citric sol-gel method containing citric acid as a chelating agent in precursor solutions. The prepared phosphors have shown strong RO emission at 600 nm corresponding to the $^4\text{G}_{5/2} \rightarrow ^6\text{H}_{7/2}$ transition of Sm^{3+} with intense excitation wavelength at 402 nm, which is close to the emission wavelength of n-UV LED. Powders sintered at 1000 °C with 3 mol% of Sm^{3+} were found to exhibit efficient RO emission from $\text{Ca}_3\text{Y}_2\text{Si}_3\text{O}_{12}$ phosphor. Based on the obtained results, we suggest that these phosphors are novel optical materials and a potential substitute for red phosphors in fabrication of efficient WLED's.

Acknowledgement

This work was supported by the Korea Research Foundation Grant funded by the Korean Government (NRF-2010-0029634) and also this work was partially supported by the Korea Research Foundation Grant funded by the Korean Government (NRF-2010-0023034).

References

- [1] H.A. Hoppe, Recent developments in the field of Inorganic phosphors, *Angew. Chem. Int. Ed.* 48 (2009) 3572–3582.
- [2] K.K. Nanda, S.C. Vanithakumari, A one step method for the growth of Ga_2O_3 -nanorod based white light emitting phosphors, *Adv. Mater.* 21 (2009) 3581–3584.
- [3] S. Nakamura, G. Fasol, *The Blue Laser Diode: GaN Based Light Emitters and Lasers*, Springer, Berlin, 1997.
- [4] Y.C. Chang, C.H. Liang, S.A. Yan, Y.S. Chang, Synthesis and photoluminescence characteristics of high color purity and brightness $\text{Li}_3\text{Ba}_2\text{Gd}_3(\text{MoO}_4)_8:\text{Eu}^{3+}$ red phosphors, *J. Phys. Chem. C* 114 (2010) 3645–3652.
- [5] K. Hwang, S. Hwangbo, J. Kim, Sol-gel synthesis of red-emitting LiEuW_2O_8 powder as a near-ultraviolet convertible phosphor, *Ceram. Int.* 35 (2009) 2517–2519.
- [6] V.R. Bandi, K. Jang, H.S. Lee, S.S. Yi, J.H. Jeong, Synthesis and photoluminescence characterization of RE^{3+} ($=\text{Eu}^{3+}, \text{Dy}^{3+}$)-activated $\text{Ca}_3\text{La}(\text{VO}_4)_3$ phosphors for white light-emitting diodes, *J. Alloys Compd.* 496 (2010) 251–255.
- [7] X.H. He, M.Y. Guan, J.H. Sun, N. Lian, T.M. Shang, Synthesis and photoluminescence properties of $\text{LiEu}(\text{W},\text{Mo})_2\text{O}_8:\text{Bi}^{3+}$ red emitting phosphor for white-LEDs, *J. Mater. Sci.* 45 (2010) 118–123.
- [8] L. Zhou, L. Yi, R. Sun, F. Gong, J. Sun, A potential red phosphor $\text{Na}_{0.5}\text{Gd}_{0.5}\text{MoO}_4:\text{Eu}^{3+}$ for light emitting diode application, *J. Am. Ceram. Soc.* 91 (2008) 3416–3418.
- [9] E. Ozel, H. Yurdakul, S. Turan, M. Ardit, G. Cruciani, M. Dondi, Co-doped willemite ceramic pigments: Technological behaviour, crystal structure and optical properties, *J. Eur. Ceram. Soc.* 30 (2010) 3319–3329.
- [10] A. Yamane, T. Kunimoto, K. Ohmi, T. Honma, H. Kobayashi, Luminescent properties of Tb-activated rare-earth oxyapatite silicate $\text{MLn}_4\text{Si}_3\text{O}_{13}$ ($\text{M}=\text{Ca},\text{Sr}, \text{Ln}=\text{La}, \text{Gd}$), *Phys. Stat. Sol. C* 3 (2006) 2705–2708.
- [11] H. Yamane, T. Nagasawa, M. Shimada, T. Endo, $\text{Ca}_3\text{Y}_2(\text{SiO}_4)_3$, *Acta Cryst. C* 53 (1997) 1367–1369.
- [12] B. Zhaohui, B. Xuewei, J. Ru, L. Bo, X. Zhiyi, Z. Xiyan, Preparation and Characterization of Bismuth Silicate Nanopowders, *Front. Chem. China* 2 (2007) 1–4.
- [13] X.M. Han, J. Lin, M.I. Pang, M. Yu, S.B. Wang, Sol-Gel Deposition and Luminescence Properties of Lanthanide Ion-Doped $\text{Y}_{2(1-x)}\text{Gd}_{2x}\text{SiWO}_8(0x1)$ Phosphor Films, *Appl. Phys. A* 80 (2005) 1547–1552.
- [14] Y. Liangzhun, F. Min, L. Yuejiao, L. Chao, W. Xiuying, Y. Xibin, Preparation and Properties of Luminous Materials of $\text{CaSiO}_3:\text{Pb}, \text{Mn}$ by Sol-Gel Method, *Front. Chem. China* 2 (2007) 442–446.
- [15] M. Yu, J. Lin, Y.H. Zhou, S.B. Wang, H.J. Zhang, Sol-Gel Deposition and luminescent properties of oxyapatite $\text{Ca}_2(\text{Y},\text{Gd})_8(\text{SiO}_4)_6\text{O}_2$ phosphor films doped with rare-earth and lead ions, *J. Mater. Chem.* 12 (2002) 86–91.
- [16] B. Vengalarao, U. Rambabu, S. Buddhudu, Emission analysis of $\text{Sm}^{3+}:\text{Ca}_4\text{GdO}(\text{BO}_3)_3$ powder phosphor, *Mater. Lett.* 61 (2007) 2868–2871.
- [17] W.T. Carnall, P.R. Fields, K. Rajnak, Electronic energy levels in the trivalent lanthanide aquo ions, *J. Chem. Phys.* 49 (1968) 4424–4442.
- [18] A. Thulasiramudu, S. Buddhudu, Optical characterization of Sm^{3+} and $\text{Dy}^{3+}:\text{ZnO-PbO-B}_2\text{O}_3$ glasses, *Spectrochim. Acta A* 67 (2007) 802–807.
- [19] K. Mini Krishna, G. Anoop, M.K. Jayaraj, Host sensitized white luminescence from $\text{ZnGa}_2\text{O}_4:\text{Dy}^{3+}$ phosphor, *J. Electrochem. Soc.* 154 (2007) J310–J313.